



PVDF– TiO₂ Composite as a Corrosion Inhibitor for Mild Steel in 3.5% NaCl

¹S. Devikala, ²P. Kamaraj and ³M. Arthanareeswari

Department of Chemistry, SRM University, Kattankulathur-603 203, Tamil Nadu, India.

Email: ¹sdevikala@gmail.com, ²kamaraj97@yahoo.co.in, ³arthanareeswari@gmail.com

[Received: 11th Nov. 2014; Accepted: 26th Nov. 2014]

Abstract— The inhibitive action of PVDF – TiO₂ (PVDTi) composite on the corrosion of mild steel in 3.5% NaCl has been investigated by potentiodynamic polarization, and electrochemical impedance spectroscopic (EIS) studies. Characterization of PVDTi composite has been carried out using Fourier transform infrared spectroscopy (FTIR) and X ray diffraction. Experimental results reveal that PVDTi composite acts as an inhibitor in 3.5% NaCl environment. The inhibition efficiency increases with an increase in the concentration of the TiO₂. Maximum inhibition efficiency of PVDTi composite was found for the highest concentration of TiO₂.

Keywords: Corrosion, PMMA, Polymer composite, FTIR spectroscopy, Electrochemical studies

I. INTRODUCTION

Valuable metals, such as mild steel, aluminum and copper are prone to corrosion when they are exposed to aggressive media (1). Therefore, there is a need to protect these metals against corrosion. It is a serious problem in the oil, fertilizer, and other industries (2-5). Therefore, there is a need to protect these metals against corrosion. The use of polymers as corrosion inhibitors have drawn considerable attention recently due to their inherent stability and cost effectiveness. Owing to the multiple adsorption sites, polymeric compounds adsorb more strongly on the metal surface compared with their monomer analogues (6-7). Therefore, it is expected that the polymers will be better corrosion inhibitors. The literature reveals that a wide range of polymeric compounds have been successfully investigated as potential inhibitors for the corrosion of metals in aggressive media. Water soluble conducting polymer composite, poly(vinyl alcohol-threonine) was chemically synthesized and the corrosion inhibition performance was evaluated (8). Titanium dioxide (TiO₂) has traditionally received a lot of attention due to its chemical stability, non-toxicity, low cost and other advantages. As a result, it is widely used as a white pigment, gas sensor, anti-reflection coating in many thin-film optical devices,

biomaterials and catalyst/support/additive in catalytic reactions (9). In continuation of our quest for developing corrosion inhibitors with high effectiveness and efficiency, the present paper aims at the utilization of PVDTi composite as corrosion inhibitor by potentiodynamic polarization and electrochemical impedance studies. FTIR and XRD spectroscopic technique was used to reveal the formation of PVDTi composites.

II. EXPERIMENTAL

Chemicals and reagents

Titanium dioxide (TiO₂), Dimethyl formamide and PVDF from Merck chemicals.

PVDF– TiO₂ composite preparation (PVDTi composite)

A definite quantity of PVDF was dissolved in dimethyl formamide followed by the addition of a known quantity of TiO₂ and then it was made into a paste in an agate mortar and was subjected to heat at 80 °C for 30 minutes in a hot air oven and made into a powder. PVDTi composites were prepared in the following proportions of PVDF and TiO₂: PVDTi 1 – 9:1, PVDTi 2 – 8:2, PVDTi 3 – 7:3, PVDTi 4 – 6:4, PVDTi 5 – 5:5 and PVDTi 6 – 4:6.

XRD

In order to understand the properties of composite material, it is essential to know about the details of its structure. The X-ray diffraction pattern (XRD) technique was used for characterization. The XRD of PVDF, TiO₂ and PVDTi composites were recorded using Philips X'PERT PRO diffractometer with Cu K α (λ = 1.54060 Å) incident radiation. The XRD peaks were recorded in the 2 θ range of 20–80°.

FTIR spectra

The FTIR spectrums of PVDF, TiO₂ and PVDTi composites were recorded using Shimadzu FTIR spectrophotometer in the range of 4000-500 cm⁻¹.

Electrochemical measurements

The experiments were performed in a classical three-electrode electrochemical cell. Mild steel specimen of 1 cm^2 area was used as the working electrode and platinum electrode as a counter electrode and saturated calomel electrode as a reference electrode. Prior to each experiment the working electrode surface was polished with emery paper. Biologic Electrochemical work station (model SP 300) interface with EC lab software were used for data acquisition and analysis. For polarization and impedance studies the period of immersion was for 30 minutes. Polarization technique was carried out from a cathodic potential of -250 mV to an anodic potential of $+250\text{ mV}$ with respect to OCP at a scan rate of 1 mV/s . In EIS technique a small amplitude AC signal of 10 mV and a frequency spectrum from 10^5 to 10^{-2} Hz was impressed at the OCP and the impedance data were analysed using Nyquist plots. The impedance data were fit into appropriate equivalent electrical circuit using EC lab software. The parameters obtained from the best fit equivalent circuit were analysed.

III. RESULTS AND DISCUSSION

XRD

The XRD pattern of pure PVDF is shown in figure 1 which indicates PVDF has monoclinic structure. The peak positions ($2\theta = 18.48(0\ 2\ 0)$, $20.18(1\ 1\ 0)$, $26.60(0\ 2\ 2)$, $34.91(1\ 3\ 1)$, $38.81(0\ 4\ 1)$ and $41.41^\circ(2\ 2\ 1)$ and relative intensities obtained for the polymer match with the JCPDS Card no. 38-1638 file, identifying it as PVDF with monoclinic structure with β phase (Figure 1). The average crystallite size is found to be $0.1549\ \mu\text{m}$.

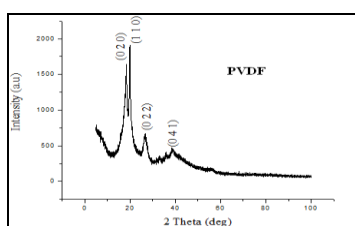


Figure 1 XRD pattern of PVDF

The peak positions ($2\theta = 25.30(1\ 0\ 1)$, $38.57(1\ 1\ 2)$, $48.04(2\ 0\ 0)$, $53.88(1\ 0\ 5)$, $62.68(2\ 0\ 4)$, $70.29(2\ 2\ 0)$, $75.05(2\ 1\ 5)$ and $83.16^\circ(3\ 1\ 2)$ and relative intensities obtained for TiO_2 match with the JCPDS Card no. 78-2486 file, identifying it as TiO_2 with anatase phase (Figure 2). The average crystallite size is found to be $0.1858\ \mu\text{m}$.

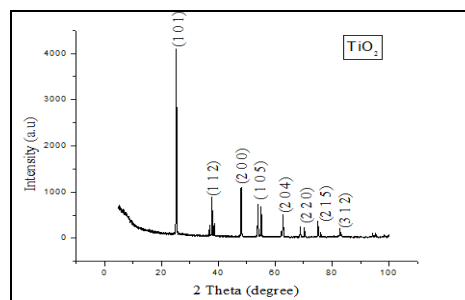


Figure 2 XRD pattern of TiO_2

The sharp crystalline diffraction peaks noticed in pure PVDF, have become less prominent in case of composites. The intensity of the peak at 38.0° , is gradually decreased (Figure 3(i) – (iii)). The occurrence of decrease in intensity of diffraction peaks with TiO_2 , suggest the decrease in the degree of crystallinity of PVDF. It is interesting to note that the PVDTi 6 is more amorphous thus leading to a higher conductivity. These observations appear to reveal that the polymer undergoes a significant structural reorganization due to the presence of the chosen TiO_2 (10). The average crystallite size is found to be $0.1409\ \mu\text{m}$. Intense peaks of PVDF found at 18.48 , 20.18 , 26.60 and 38.81° are remarkably reduced for the composites. Crystallinity of the host polymer is disrupted by the addition of TiO_2 and it can be attributed to destruction of the ordered arrangement of the polymer side chains. The segmental mobility of polymer chains is much higher in amorphous regions than in the crystalline region. The amorphous nature produces greater ionic diffusivity in accordance with the ionic conductivity (11). In general, a decrease in the crystalline nature effectively increases the flexibility of the polymeric backbone and promotes the ion transfer. The observed decrease in FWHM (Full width half maximum) and decrease in crystallite size is generally associated with decrease in the crystallinity of polymer composites (12). After the introduction of TiO_2 into the polymer chains, a slight shift in the strongest peak position to lower angle is observed, indicating the presence of specific interactions between PVDF and TiO_2 . The average crystallite size is found to be $0.1358\ \mu\text{m}$.

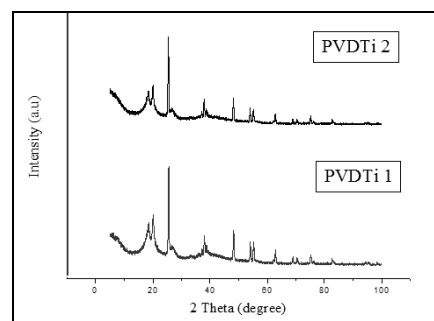


Figure 3(i) XRD patterns of PVDTi 1 and 2

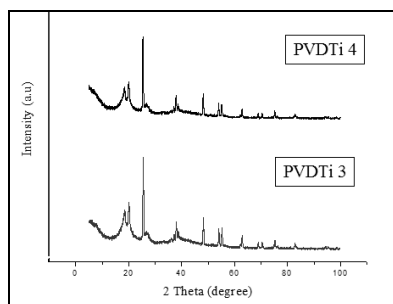


Figure 3(ii) XRD patterns of PVDTi 3 and 4

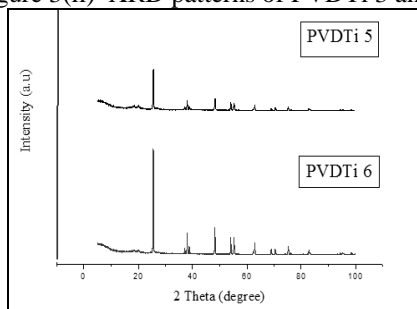


Figure 3(iii) XRD patterns of PVDTi 5 and 6

FTIR

The observed vibrational band at 1402 cm^{-1} belongs to the deformation vibration of the CH_2 group. The peaks noticed at 873 and 854 cm^{-1} belongs to the rocking mode of vinylidene group of the polymer. The band at 1066 cm^{-1} is due to β crystalline phase of PVDF (Figure 4). The bands at 532 and 498 cm^{-1} may be assigned to the wagging and bending vibration of CF_2 . The bending vibration of CF_2 is observed at 613 cm^{-1} also (13-14).

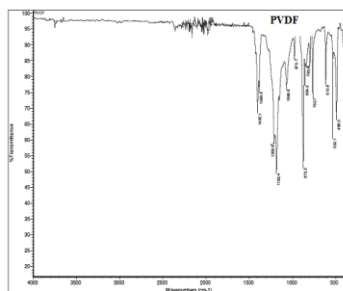
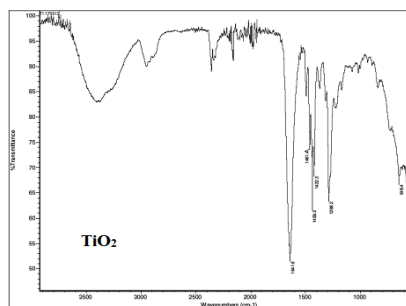


Figure 4 FTIR spectrum of PVDF

In the FTIR spectrum of TiO_2 , Ti-O bands in the range of $800\text{-}450\text{ cm}^{-1}$ corresponds to the stretching mode vibration of Ti-O and the peak at 511 cm^{-1} , the characteristic of Ti-O anatase crystalline phase (15). The peaks at 550 and 1479 cm^{-1} corresponds to the stretching vibration of Ti-O and Ti-O-Ti respectively (Figure 5).

Figure 5 FTIR spectrum of TiO_2

The bands between 1060 and 1000 cm^{-1} in the composite PVDTi show the characteristic peaks of TiO_2 . A band at 511 cm^{-1} is due to stretching vibration of Ti-O in the composite (Figure 6(i) – (iii)). A peak at 491 cm^{-1} indicates the presence of Ti-O-Ti stretching vibration in the composite. In addition, the bands occurring between $800\text{-}1400\text{ cm}^{-1}$ are due to the lattice vibrations of TiO_2 in the composite. The characteristic PVDF peaks such as 1401 , 1184 , 1929 cm^{-1} and the bands between $2400\text{-}2014\text{ cm}^{-1}$ are also present in the composite. It can be seen clearly that the intensity of the band at 762 cm^{-1} which is characteristic of a crystalline phase of PVDF decreases with the increase of TiO_2 content, implying the interaction between PVDF and TiO_2 . It is very note worthy that PVDF remain in small traces, in the polymer composites with high TiO_2 content. This is unique phenomenon when comparing with anatase TiO_2 , whose higher anatase TiO_2 content easily destroys the crystalline phase of PVDF (16).

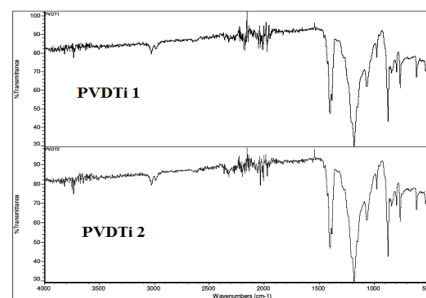


Figure 6 (i) FTIR spectra of PVDTi 1 and 2

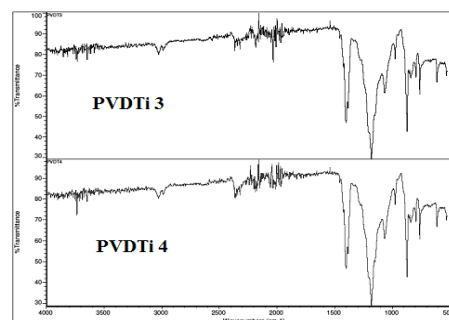


Figure 6 (ii) FTIR spectra of PVDTi 3 and 4

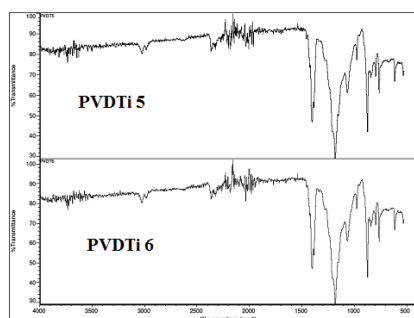


Figure 6 (iii) FTIR spectra of PVDTi 5 and 6

Polarization studies

The I_{corr} of bare mild steel is $35.1 \mu\text{A}/\text{cm}^2$. The incorporation of TiO_2 into PVDF matrix reduced the corrosion currents of PVDTi 60.9 and $2.0 \mu\text{A}/\text{cm}^2$. This indicates that the addition of ceramic oxides in PVDF matrix has improved the corrosion resistance. It is seen that the least corrosion current value i.e. a better corrosion resistance is displayed by PVDTi 6 (Figure 7). The corrosion potential E_{corr} of bare mild steel is -706 mV . The incorporation of TiO_2 into PVDF matrix resulted in a positive shift in potential. This indicates that the addition of ceramic oxides in PVDF matrix has improved the corrosion resistance. An increase in ceramic oxides content in the composites PVDTi 6, resulted in a significant shift to more positive value indicating its better corrosion resistance behaviour compared to all the other 5 composite samples (Table 1). Thus, it's understood that the addition of ceramic oxides upto 10-60 wt% favours the corrosion resistance (17). This indicates that with increase in the content of ceramic oxides, the corrosion rate decreases.

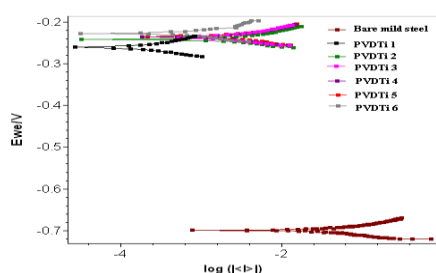


Figure 7 Potentiodynamic polarization curves for mild steel in 3.5% NaCl in absence and presence of different concentration of PVDTi composites

Table 1 Corrosion parameters obtained from Polarization studies for bare mild steel and coated PVDTi composites

System studied	E_{corr} (mV)	I_{corr} ($\mu\text{A}/\text{cm}^2$)	Corrosion rate (mpy)
Bare mild steel	-706	35.1	10.72
PVDTi 1	-264	10.2	3.11
PVDTi 2	-247	8.5	2.59

PVDTi 3	-243	6.1	1.86
PVDTi 4	-241	4.9	1.49
PVDTi 5	-239	2.6	0.79
PVDTi 6	-235	0.9	0.28

EIS Studies

The Nyquist plots of composites with different oxides are shown in the figures 8. Figures represent the Nyquist plot. The interception of Z' in the nyquist plot at higher frequencies is ascribed as electrolytic bulk resistance R_s and at lower frequencies the interception is ascribed as R_{ct} . The Nyquist plot shows the emergence of a second semi circle. The equivalent circuit (Figure 9 and 10) used for fitting the plots obtained for bare mild steel and coatings and the fitted values are displayed in Table 2. The R_{ct} values increased significantly when compared to bare mild steel. The R_{ct} value being the highest for PVDTi 6 indicating that the active area available for corrosive attack is less or alternatively the corrosion resistance is better compared to other samples(18). It is understood from the table that C_{dl} value is very low for PVDTi 6. This indicates that addition of around 60 wt% of ceramic oxide improved the surface morphology of the coating and decreased the surface defects. The improvement of corrosion resistance could be attributed to the fine surface structure of composite coating compared to bare mild steel due to the incorporation of ceramic oxide particles into polymer (19-21). The higher values of the R_{ct} obtained for the composite coatings of the present study imply better corrosion protective ability (22).

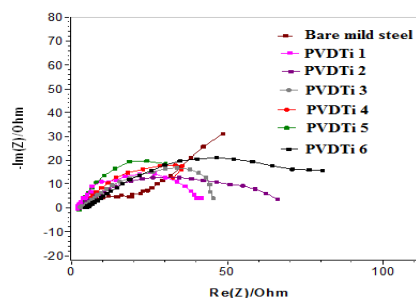


Figure 8 Nyquist plots for bare mild steel and PVDTi composites

Table 2 Electrochemical parameters obtained from Impedance studies for bare mild steel and coated PVDTi composites

System studied	R_{ct} (Ohm cm^2)	C_{dl} (μF)
Bare mild steel	23.4	2.583×10^{-2}
PVDTi 1	41.25	2.530×10^{-3}
PVDTi 2	57.16	2.010×10^{-3}
PVDTi 3	62.44	1.980×10^{-3}
PVDTi 4	65.77	1.121×10^{-3}
PVDTi 5	68.61	1.080×10^{-3}
PVDTi 6	99.11	0.786×10^{-3}

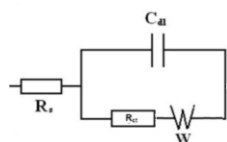


Figure 9 Equivalent circuit model for bare mild steel

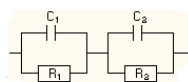


Figure 10 Equivalent circuit model for PVDF composites

IV. CONCLUSIONS

PVDF– TiO₂ (PVDTi) composite acted as an effective corrosion inhibitor for mild steel in 3.5% NaCl medium. PVDTi composite formation was confirmed by XRD and FTIR techniques. The inhibition efficiency of PVDTi composite increases with increase in concentration. Maximum inhibition efficiency was 94% at 60 wt % concentration of TiO₂. Electrochemical studies confirmed the mixed mode of inhibition for the corrosion of mild steel in 3.5% NaCl medium. without modifying the mechanism of hydrogen evolution of the inhibitor and dissolution of metal.

V. REFERENCES

- [1] Ebenso E.E., Eddy N.O., Oldiongenyi A.O., 2009, "Corrosion Inhibition and adsorption properties of methocarbomal on mild steel in acidic media", *Port. Electrochemical Acta* 27(1),13-22.
- [2] Eddy, N.O., Mamza, P.A.P., 2009. Inhibitive and adsorption properties of ethanol extract of seeds and leaves of *Azadirachta indica* on the corrosion of mild steel in H₂SO₄. *Port. Electrochim. Acta* 27 (4), 443–456.
- [3] Aytac, A., Ozmen, U., Kabasakaloglu, M., 2005. Investigation of some Schiff bases as acidic corrosion of alloy AA3102. *Mater. Chem. Phys.* 89 (1), 176–181.
- [4] Eddy, N.O., 2009. Ethanol extract of *Phyllanthus amarus* as a green inhibitor for the corrosion of mild steel in H₂SO₄. *Port. Electrochim. Acta* 27 (5), 579–589.
- [5] Eddy, N.O., 2010. Part 3. Theoretical study on some amino acids and their potential activity as corrosion inhibitors for mild steel in HCl. *Mol. Simul.* 36 (5), 354–363.
- [6] P. Kamaraj , S. Devikala and M. Arthanareeswari, 2014, Fabrication, Characterization and Application of Polymethylmethacrylate/Titanium dioxide Composite Coatings for corrosion inhibition, *International Journal Of Advanced scientific and technical research*, 4(1), 711-720.
- [7] S. Devikala, P. Kamaraj and M. Arthanareeswari, 2014, Electrochemical Performance of PMMA/Al₂O₃ Composite Coatings *International Journal of Advanced Chemical Science and Applications*, 1(2), 9-15.
- [8] Subhashini, S., and Ali Fathima Sabirneeza, A., 2011, "Gravimetric And Electrochemical Investigation Of Water Soluble Poly(vinyl alcohol- threonine) As Corrosion Inhibitor For Mild Steel", *Proceedings of the world congress on Engineering and Computer science Volume II W CECS October ,19-21, San Francisco, USA*,
- [9] Rao, P.G., Iwasa, M., Tanaka, T., Kondoh, I., Inoue, T., 2003, "Preparation And Mechanical Properties of Al₂O₃–15wt.%ZrO₂ Composites", *Scripta Materialia*, 48, 437–441.
- [10] Wei Li, Hong Li, Yong-Ming Zhang., "Preparation and investigation of PVDF/PMMA/TiO₂ composite film", *Journal of Materials Science*,44(11), pp. 2977-2984, 2009.
- [11] Jung Gyu Lee, Seong Hun Kim, "Structure development of PVDF/PMMA/TiO₂ composite film with casting conditions", *Macromolecular Research*, 19(1), pp. 72-78, 2011.
- [12] Weihua Tang, Tiange Zhu, Peipei Zhou, Wei Zhao, Qian Wang, Gang Feng, Huilin Yuan, "Poly(vinylidene fluoride)/poly(methyl methacrylate)/TiO₂ blown films: preparation and surface study", *Journal of Materials Science*, 46(20), pp. 6656-6663, 2011.
- [13] Hilczer, B., Kulek, J., "The Effect of Dielectric Heterogeneity on Pyroelectric Response of PVDF", *IEEE Trans. Dielectrics Electrical. Insulation* 5 (1), pp. 45–50, 1998.
- [14] Mattsson, B., Ericson, H., Torell, L.M., and Sundholm, F., "Micro-Raman Investigations of PVDF- Based Proton-Conducting Membranes", *Journal of Polymer Science, Part A: Polymer Chemistry*, 37, pp. 3317-3327, 1999.
- [15] Mriazian., and Bahari, A., "Synthesis and nanostructural investigation of TiO₂ nanorods doped by SiO₂", *Pramana Journal of physics*, 78 (2), pp. 319–331, 2012.

- [16] Wei Li, A., Hong Li, A., and Yong-Ming Zhang., "Preparation and investigation of PVDF/PMMA/TiO₂ composite film", *Journal of Material Science*, 44, pp. 2977–2984, 2009.
- [17] Meenu Srivastava., Srinivasan, A., and William Grips, V. K., "Influence of zirconia incorporation on the mechanical and chemical properties of Ni-Co alloys", *American journal of Materials science*, 1(2), pp. 113-122, 2011.
- [18] Barcia, O. E., Mattos, O. R., Pebere, N., Tribdlet, B., "Mass-Transport Study for the Electrodeposition of Copper in 1M Hydrochloric Acid Solution by Impedance", *Journal of the Electrochemical Society*, 140 (10), pp. 2825, 1993.
- [19] Feng, Y., Teo, W. K., Siow, K. S., Tan, K. L., Hsieh, A. K., "The corrosion behaviour of copper in neutral tap water. Part I: Corrosion mechanisms", *Corrosion science*, 38 (3), pp. 369-385, 1996.
- [20] Wang, C. T., Chen, S. H., Ma, H. Y., Hua, L., Wang, N. X., "Study of the stability of self-assembled N-vinylcarbazole monolayers to protect copper against corrosion", *J serbian chemical society*, 67 (10), pp. 685-696, 2002.
- [21] Quaraishi, M. A., and Sardar, R., "Hector bases-a new class of heterocyclic corrosion inhibitors for mild steel in acid solution", *J Appl Electro chemistry*, 33(12), pp. 1163-1168, 2003.
- [22] Lebrini, M., Lagrenee, M., Vezin, H., Gengembre, L., and Bentiss, F., "Electrochemical and quantum mechanical studies of new thiadiazole derivatives adsorption on mild steel in norma HCl medium", *Corrosion science*, 47(2), pp. 485-505, 2005.

